

Electronic Supplementary Information *for*

Multiwavelength-Controlled Multicolor Photochromism and Fluorescence Switch Based on an Efficient Photocyclization Reaction by Introducing Two Photoactive Subunits into AIEgens

Qiaozhi Zhu, Jiaqi Zuo, Xinni Ping, Yuqing Zhu, Xuting Cai, Zuping Xiong, Zhaosheng Qian and Hui

Feng*

*Corresponding author. E-mail: fenghui@zjnu.cn.

Key Laboratory of the Ministry of Education for Advanced Catalysis Materials, College of Chemistry and Life Sciences, Zhejiang Normal University, Jinhua 321004, People's Republic of China

1. Experimental Section

2. Computational Details

3. Supplementary Schemes, Figures and Tables

3.1 Scheme S1. Synthesis routes of DPDBE, DPDTE, DPDFTE and DPDPTE.

3.2 Figure S1. Time-resolved PL decay curve of DPDTE in solid state.

3.3 Figure S2. PL spectra and images of DPDTE (a), DPDPTE (b) in solid state before and after UV irradiation.

3.4 Figure S3. UV-visible spectra of DPDTE, DPDFTE and DPDPTE in THF at 25.0 μM .

3.5 Figure S4. (a) Schematic illustration of photo-controlled cyclization, cycloreversion and dehydrogenation reactions of DPDFTE. (b) Comparison of ^1H NMR spectra of DPDFTE (10 mM) in CDCl_3 before and after UV irradiation.

3.6 Figure S5. PL spectra and images of DPDTE (a), DPDFTE (b) DPDPTE (c) in sucrose octaacetate film (1:50 in mass ratio) before and after UV irradiation.

3.7 Table S1. Experimental and computational data for $\text{S}_0 \rightarrow \text{S}_1$ absorption maxima and absorption coefficient of DPDTE, DPDFTE and DPDPTE and their cyclized products.

4. NMR and HRMS Spectra of Compounds

4.1 Figure S6. ^1H NMR spectrum of DPDBE in CDCl_3 .

4.2 Figure S7. ^{13}C NMR spectrum of DPDBE in CDCl_3 .

4.3 Figure S8. ^1H NMR spectrum of DPDTE in CDCl_3 .

- 4.4 Figure S9.** ^{13}C NMR spectrum of DPDTE in CDCl_3 .
- 4.5 Figure S10.** ^1H NMR spectrum of DPDFTE in CDCl_3 .
- 4.6 Figure S11.** ^{13}C NMR spectrum of DPDFTE in CDCl_3 .
- 4.7 Figure S12.** ^1H NMR spectrum of DPDPTE in CDCl_3 .
- 4.8 Figure S13.** ^{13}C NMR spectrum of DPDPTE in CDCl_3 .
- 4.9 Figure S14.** High-resolution mass spectrum of DPDBE.
- 4.10 Figure S15.** High-resolution mass spectrum of DPDTE.
- 4.11 Figure S16.** High-resolution mass spectrum of DPDFTE.
- 4.12 Figure S17.** High-resolution mass spectrum of DPDPTE.
- 5. Reference**

1. Experimental Section

Synthesis of ((Z)-(1,2-diphenyl)-(Z)-di(4,4,5,5-tetramethyl-1,3,2-dioxaborolan-2-yl)ethene (DPDBE). A mixture of tetrakis(triphenylphosphine)platinum ($\text{Pt}(\text{PPh}_3)_4$) (0.18 g, 1 mol%), bis(pinacolato)diboron (7.20 g, 27.77 mmol) and 1,4-diphenylacetylene (2.47 g, 13.9 mmol) were added in DMF (70 mL) under the protection of N_2 , and the mixture was heated at 90 °C for 24 h. After the reaction was completed, the mixture was poured into water and extracted three times with dichloromethane, and then the organic layer was dried by MgSO_4 . The solvent was removed under reduced pressure. DPDBE (2.5 g) was obtained by washing several times with ethanol as a white solid with a yield of 42%. Molecular formula: $\text{C}_{26}\text{H}_{34}\text{B}_2\text{O}_4$. ^1H NMR (600 MHz, CDCl_3) δ (ppm) 7.08-7.01 (m, 6H), 6.95-6.94 (d, $J = 6$ Hz, 4H), 1.32 (s, 24H). ^{13}C NMR (150 MHz, CDCl_3) δ (ppm) 141.37, 129.43, 127.55, 125.91, 84.20, 25.01. HRMS (EI) m/z : $[\text{M}+\text{H}]^+$ 433.2735 (calcd. 432.2643).

Synthesis of (Z)-1,2-diphenyl-1,2-di(thiophen-3-yl)ethene (DPDTE). A mixture of (Z)-1,2-diphenyl-1,2-bis(4,4,5,5-tetramethyl-1,3,2-dioxaborolan-2-yl)ethane (DPDBE) (4.32 g, 10 mmol), 3-bromothiophene (3.26 g, 20 mmol) and 2M potassium carbonate (10 mL), $\text{Pd}(\text{PPh}_3)_4$ (17.33 mg, 0.015 mmol) were added in a mixed solvent containing THF (20 mL) and toluene (10 mL) under the protection of N_2 , and then the mixture was heated at 80 °C for 8 h. After the reaction was completed, the mixture was poured into water and extracted three times with dichloromethane, and then the organic layer was dried by MgSO_4 . The solvent was removed under reduced pressure and purified by silica gel column chromatography. The final crude product was recrystallized in ethanol to produce a white solid with a yield of 50.8%. Molecular formula: $\text{C}_{22}\text{H}_{16}\text{S}_2$. ^1H NMR (600 MHz, CDCl_3): δ 7.11-7.08 (m, 8H), 7.05-7.03 (m, 4H), 6.86 (d, $J = 3.0$, 2H), 6.69 (d, $J = 5.0$, 2H); ^{13}C NMR (150 MHz, CDCl_3): δ 144.46, 143.26, 135.45, 131.18, 129.91, 127.73, 126.62, 125.64, 124.17; MS (EI) m/z : $[\text{M}]^+$, 344.0 (calcd. for $\text{C}_{22}\text{H}_{16}\text{S}_2$, 344.0).

Synthesis of (Z)-1,2-diphenyl-1,2-di(2-formylthiophen-4-yl)ethene (DPDFTE).

The synthesis of DPDFTE followed the procedure of DPDTE by replacing 3-bromothiophene with 4-bromothiophene-2-carboxaldehyde. The crude product was finally acquired by recrystallization in ethanol to give a white solid with a yield of 58.4%. Molecular formula: $C_{24}H_{16}O_2S_2$. 1H NMR (600 MHz, $CDCl_3$): δ 9.76 (s, 2H), 7.38 (s, 2H), 7.33 (s, 2H), 7.15-7.13 (m, 6H), 7.03-7.01 (m, 4H); ^{13}C NMR (150 MHz, $CDCl_3$) δ 183.95, 145.05, 143.52, 141.65, 138.44, 135.38, 135.27, 130.90, 128.23, 127.54; HRMS (ESI) m/z : $[M+H]^+$, 401.0666 (calcd. for $C_{24}H_{16}O_2S_2$, 400.0592).

Synthesis of (Z)-1,2-diphenyl-1,2-di(5-((Z)-2-cyano-2-phenylvinyl)-thiophen-4-yl)ethene (DPDPTE). A certain amounts of (Z)-4,4'-(1,2-diphenylethene-1,2-diyl)bis(thiophene-2-carbaldehyde) (DPDFTE) (1.79 g, 3.0 mmol), phenylacetonitrile (0.53 g, 4.5 mmol) and sodium ethoxide (5 mL, 20% W/W) were dissolved in ethanol (30 mL), and the mixture was refluxed for 4 h. After removing the solvent under reduced pressure, the residue was purified by silica gel chromatography using petroleum ether and dichloromethane (10:1 v/v) as eluent to obtain crude product, and then the crude product was recrystallized with ethanol to obtain the final product as light-yellow solid (yield 54.8%). Molecular formula: $C_{40}H_{26}N_2S_2$. 1H NMR (600 MHz, $CDCl_3$): δ 7.59 (m, 4H), 7.50 (s, 2H), 7.40 (t, 4H), 7.34 (t, 2H), 7.24 (s, 2H), 7.15 (s, 2H), 7.14-7.13 (m, 6H), 7.07-7.05 (m, 4H); ^{13}C NMR (150 MHz, $CDCl_3$): δ 144.53, 142.14, 137.42, 135.38, 135.30, 134.33, 133.93, 131.02, 130.53, 129.19, 129.10, 128.05, 127.23, 125.82, 118.08, 108.45; HRMS (ESI) m/z : $[M+H]^+$, 599.1595 (calcd. for $C_{40}H_{26}N_2S_2$, 598.1537).

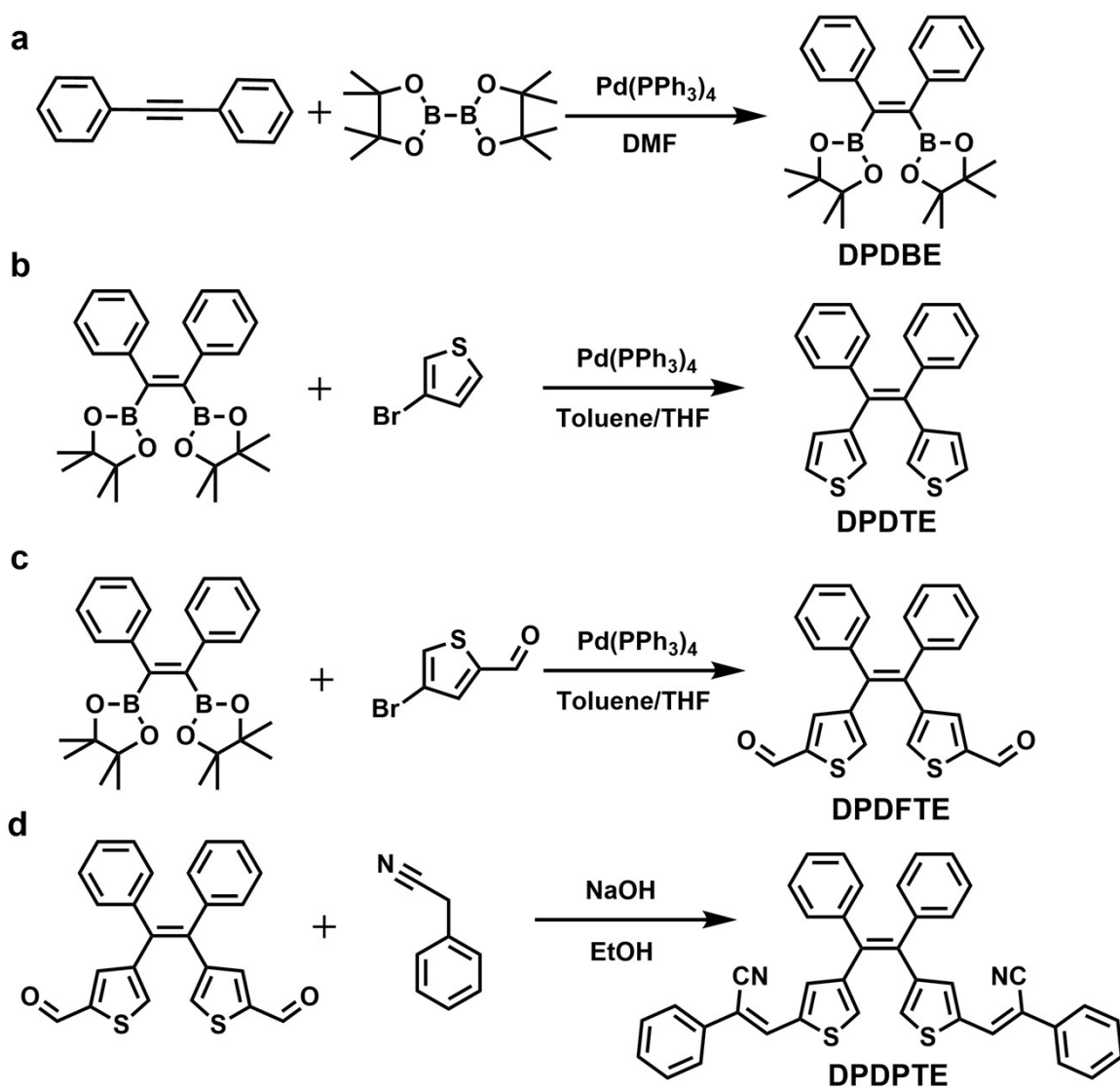
Characterization of UV-Visible and Fluorescence Properties of All Samples. UV-vis absorption spectra were recorded using an Agilent Cary 5000 UV-Vis-NIR spectrophotometer. Steady PL spectra of all samples were performed on an Edinburgh Instruments model FLS980 fluorescence spectrophotometer equipped with a xenon arc lamp using a front face sample holder. Time-resolved fluorescence measurements were conducted with EPL-series lasers. The absolute PL quantum yields of all samples were

determined using an integrating sphere equipped in FLS980 spectrophotometer for at least three times.

2. Computational Details

All the calculations were performed with density functional theory (DFT) and time-dependent density functional theory (TDDFT) implemented in Gaussian 09 program package.¹ The ground state equilibrium geometries and the normal modes of vibration of the single-molecules of DPDTE, DPDFTE, DPDPTE and their cyclized forms were computed using density functional theory (DFT) with the hybrid M062X functional at 6-311+G(d,p) level.² Excitation energies and absorption maxima of all the molecules and their cyclized products were calculated using M062X functional with 6-311+G(d,p) level based on the optimized structure in THF with SCRF.³

3. Supplementary Schemes, Figures and Tables



Scheme S1. Synthesis routes of DPDBE (a), DPDTE (b), DPDFTE (c) and DPDPTE (d).

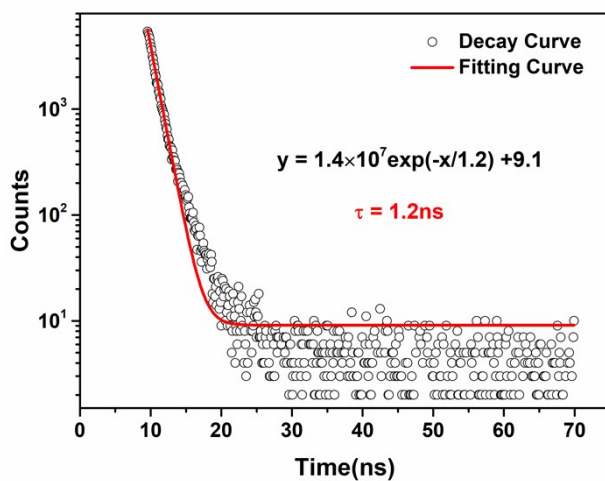


Figure S1. Time-resolved PL decay curve of DPDTE in solid state.

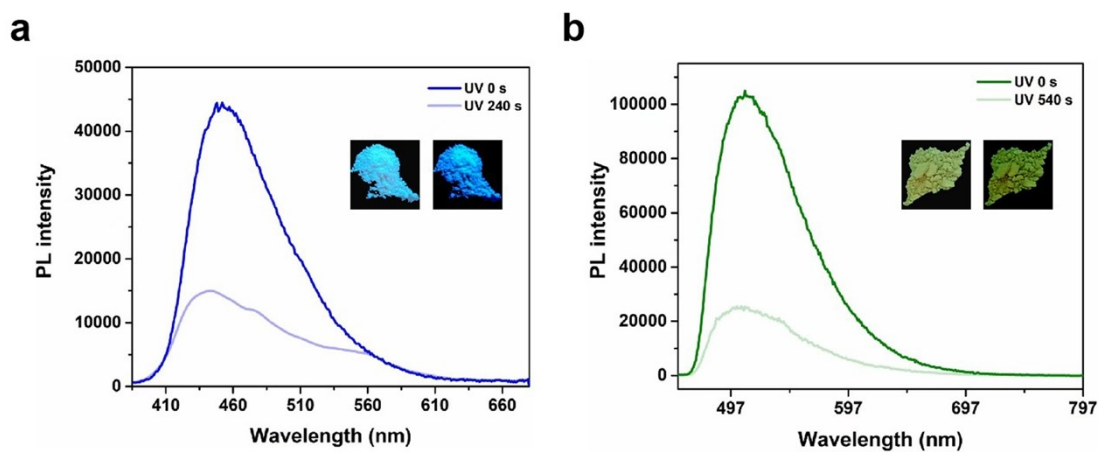


Figure S2. PL spectra and images of DPDTE (a), DPDTE (b) in solid state before and after UV irradiation.

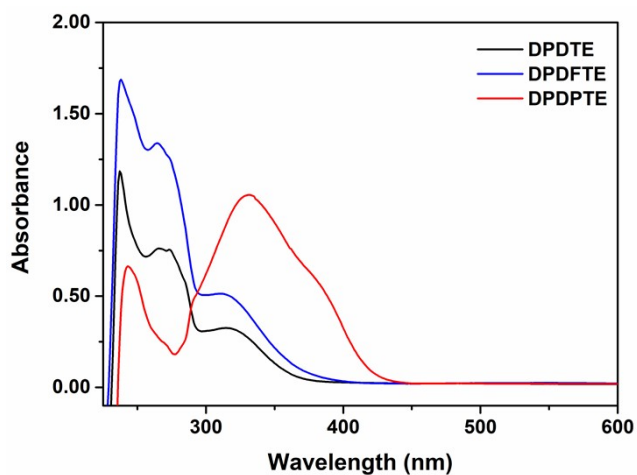


Figure S3. UV-visible spectra of DPDTE, DPDPTE and DPDPTE in THF at 25.0 μM .

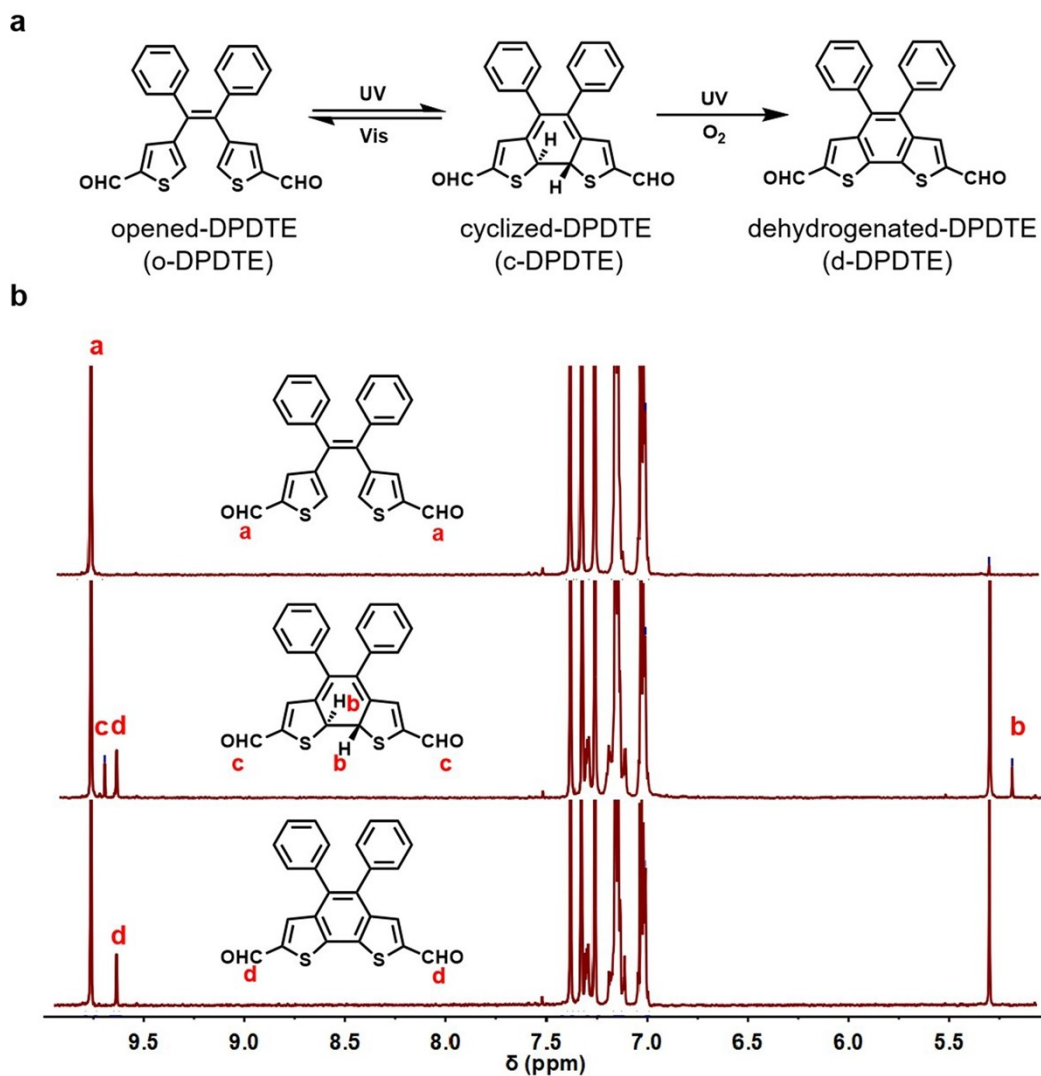


Figure S4. (a) Schematic illustration of photo-controlled cyclization, cycloreversion and dehydrogenation reactions of DPDFTE. (b) Comparison of ^1H NMR spectra of DPDFTE (10 mM) in CDCl_3 before and after UV irradiation.

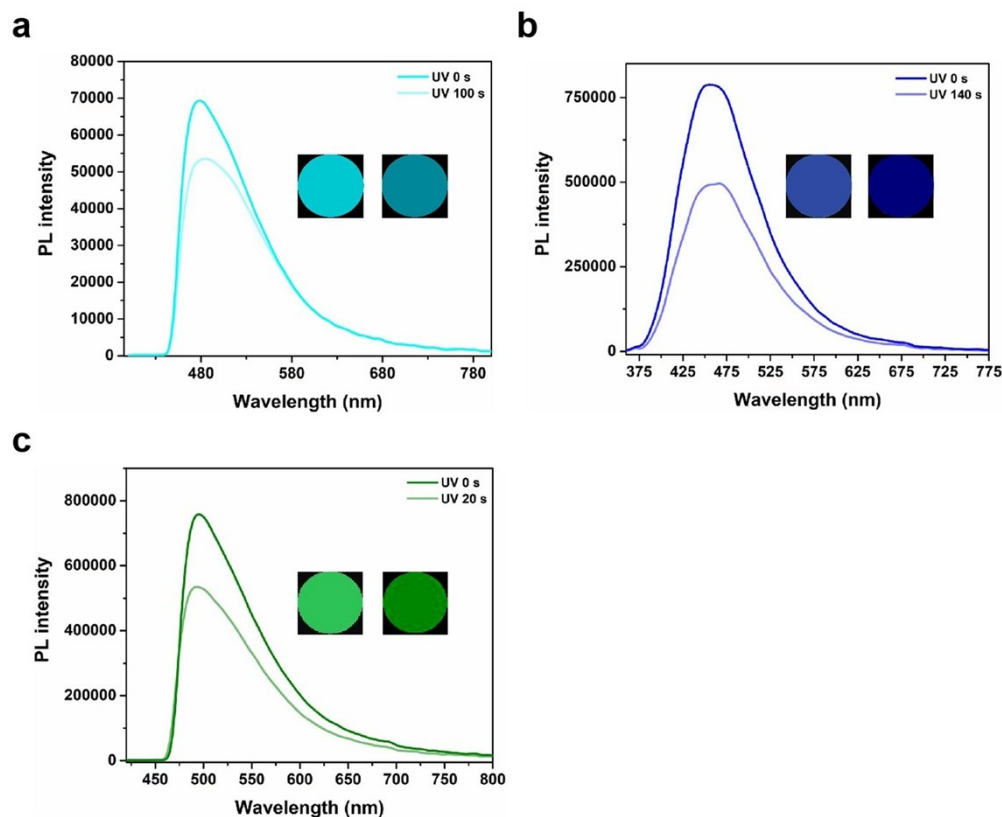


Figure S5. PL spectra and images of DPDTE (a), DPDPTE (b) DPDTE (c) in sucrose octaacetate film (1:50 in mass ratio) before and after UV irradiation.

Table S1. Experimental and computational data for $S_0 \rightarrow S_1$ absorption maxima and absorption coefficient of DPDTE, DPDPTE and DPDTE and their cyclized products.

Compounds	λ_{ab}^a (nm)	ϵ_{ab}^a ($L \cdot mol^{-1} \cdot cm^{-1}$)	λ_{ab}^b (nm)	f^b
Opened-DPDTE	314	6964	320	0.3479
Closed-DPDTE	450	-	427	0.1316
Opened-DPDPTE	310	10280	329	0.4907
Closed-DPDPTE	550	-	536	0.2509
Opened-DPDPTE	370	14587	356	0.7742
Closed-DPDPTE	650	-	613	0.6877

^{a)} The experimental data in THF with a concentration of 750.0 μM . ^{b)} The calculated values in acetonitrile with M062X functional. λ_{ab} , ϵ_{ab} and f represent absorption maximum, molar absorption coefficient and oscillator strength respectively.

4. NMR and HRMS Spectra of Compounds

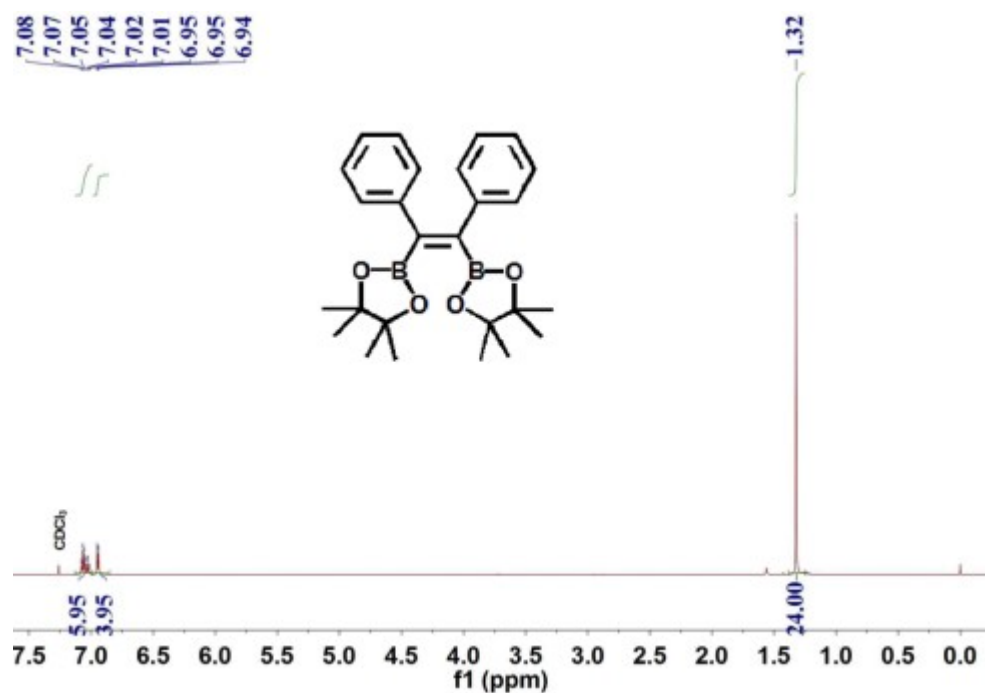


Figure S6. ^1H NMR spectrum of DPDBE in CDCl_3

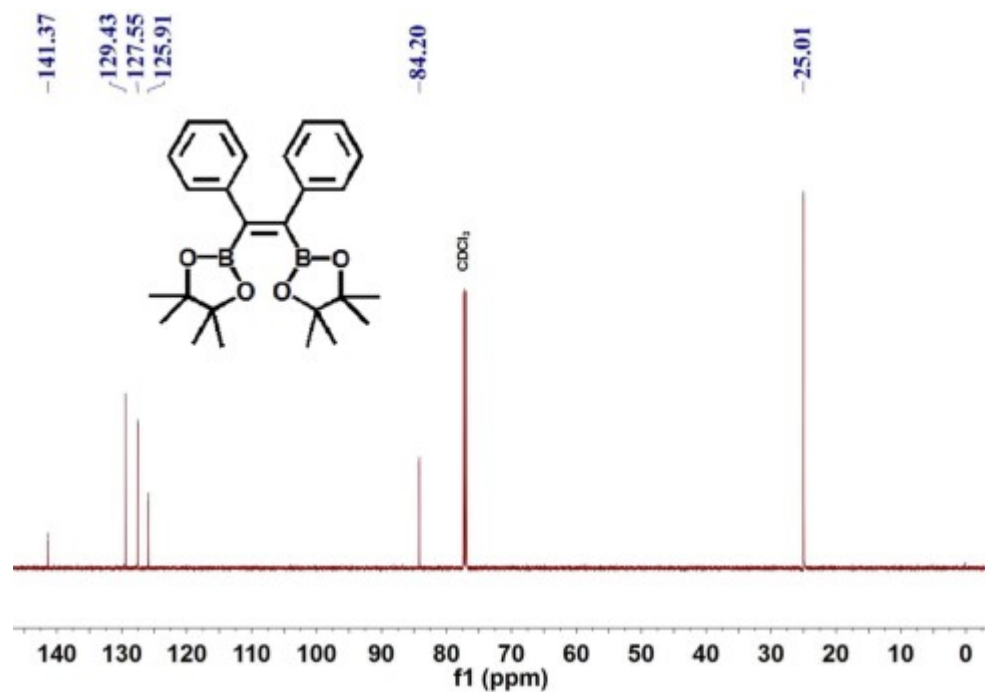


Figure S7. ^{13}C NMR spectrum of DPDBE in CDCl_3 .

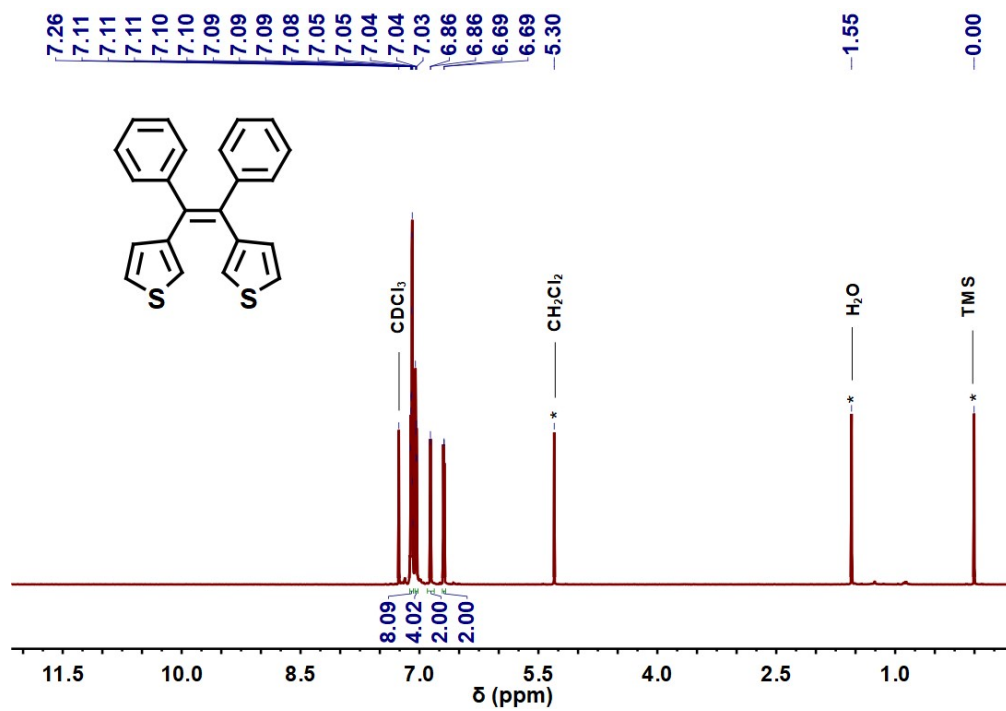


Figure S8. ¹H NMR spectrum of DPDTE in CDCl₃

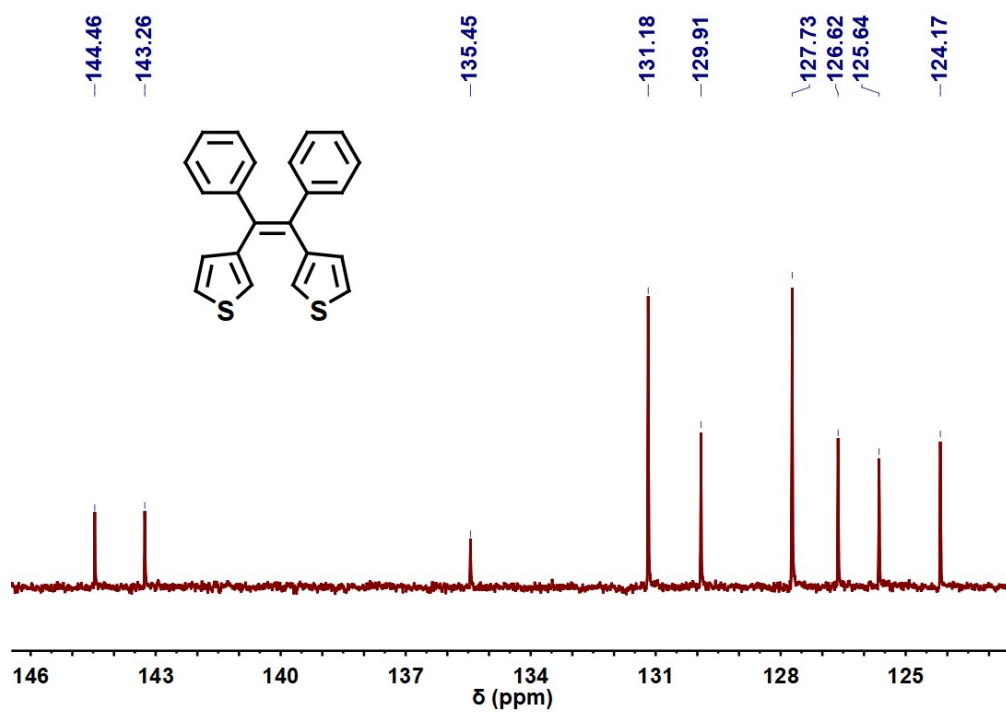


Figure S9. ¹³C NMR spectrum of DPDTE in CDCl₃.

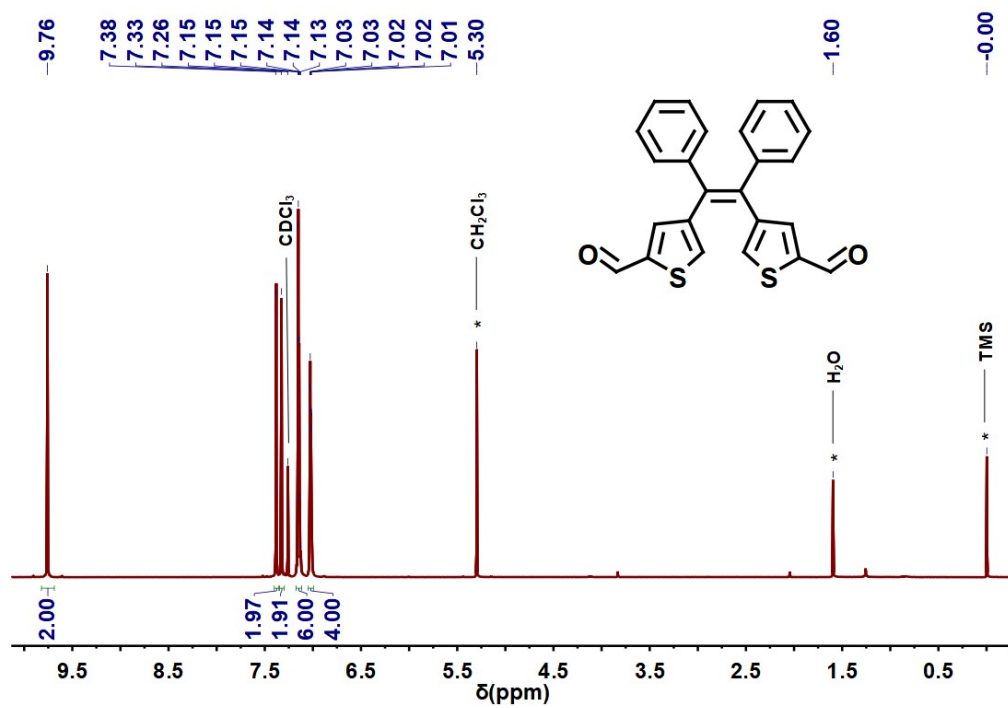


Figure S10. ^1H NMR spectrum of DPDFTE in CDCl_3 .

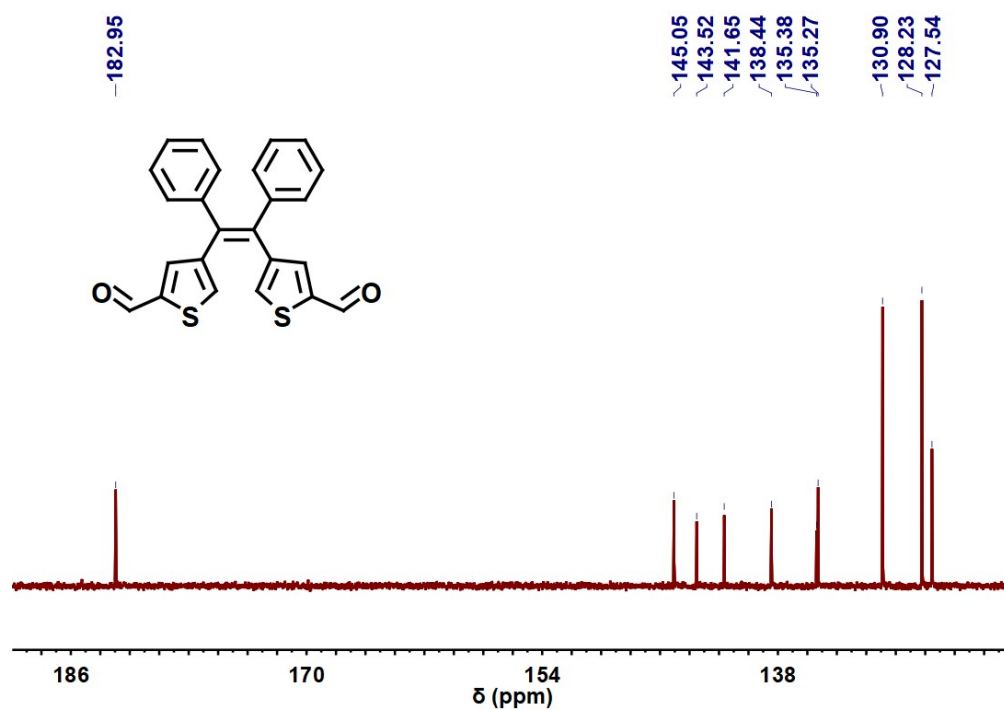


Figure S11. ^{13}C NMR spectrum of DPDFTE in CDCl_3 .

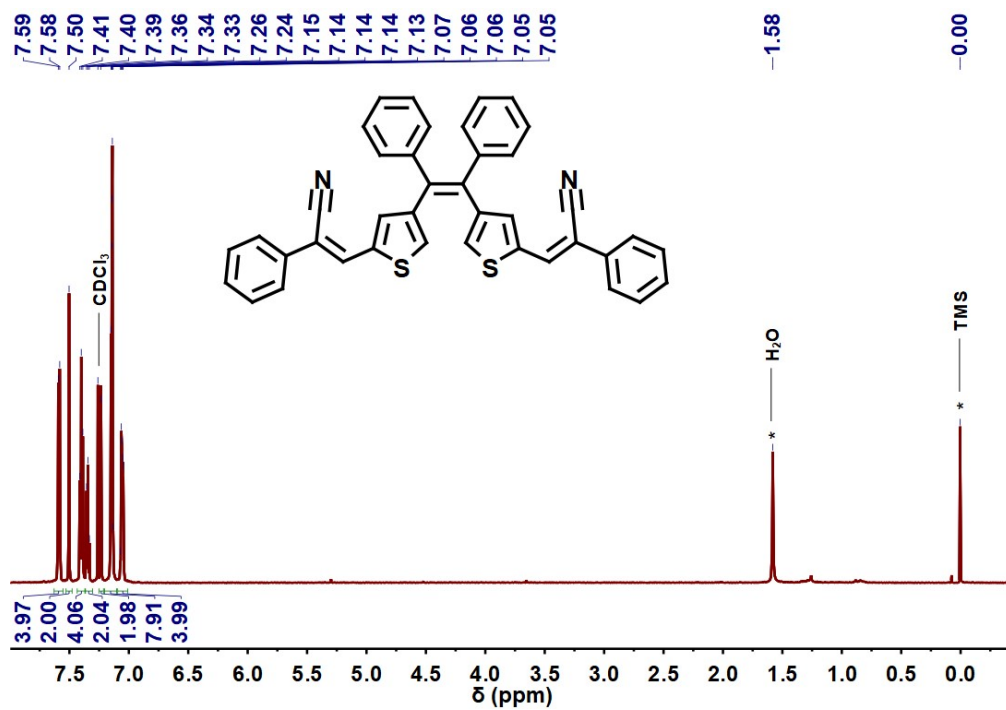


Figure S12. ¹H NMR spectrum of DPDPTe in CDCl₃.

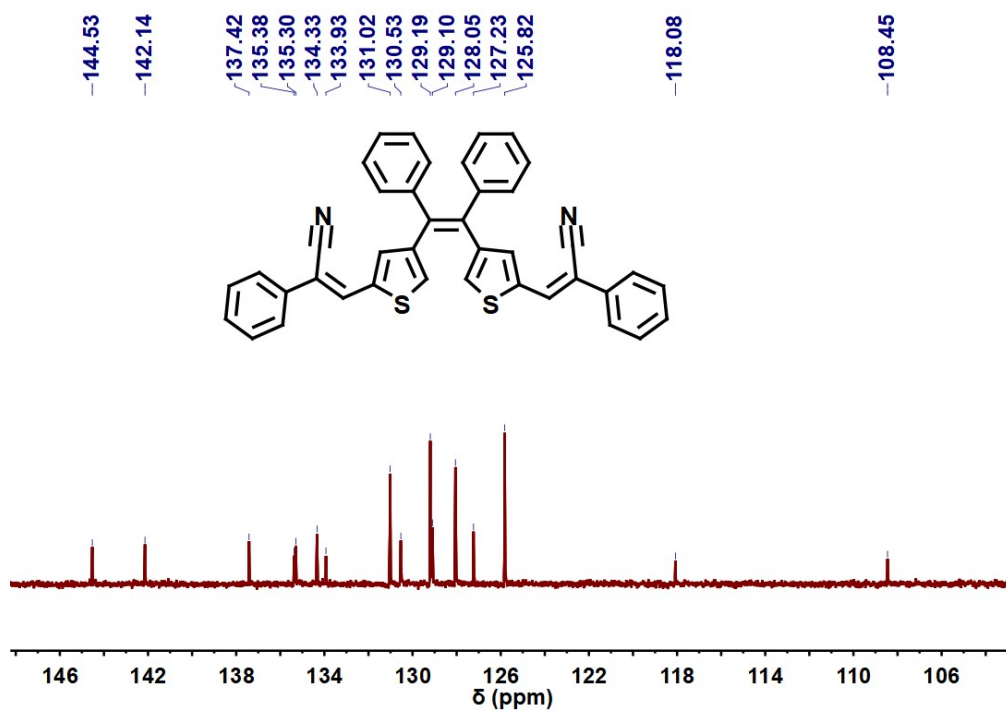


Figure S13. ¹³C NMR spectrum of DPDPTe in CDCl₃.

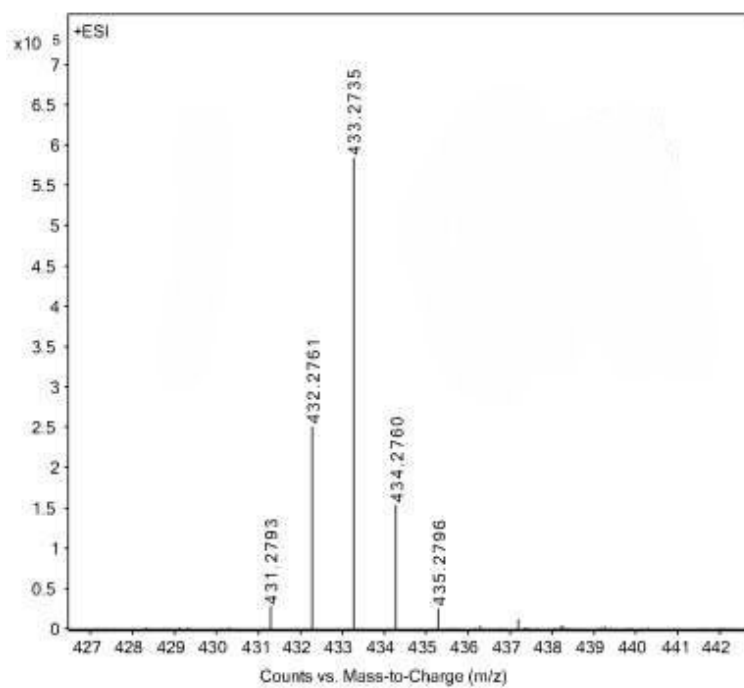


Figure S14. High-resolution mass spectrum of DPD BE.

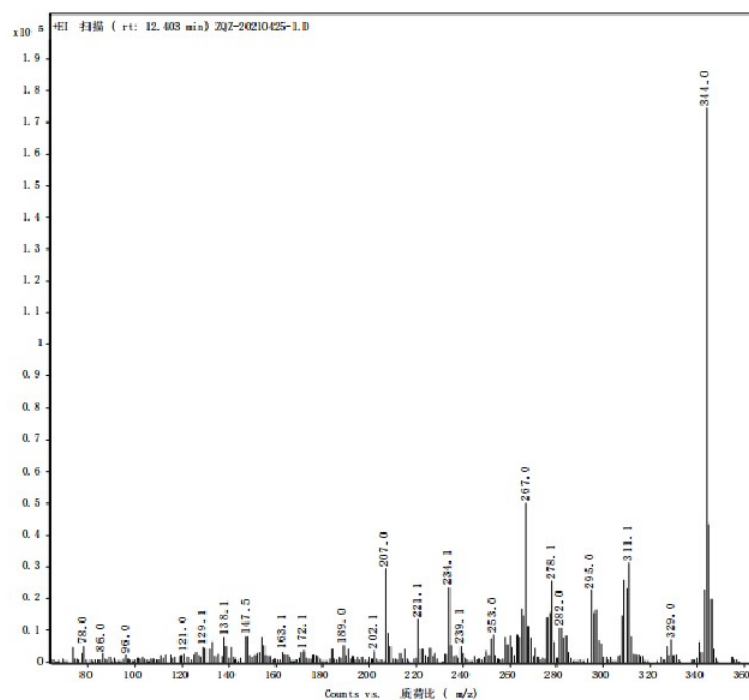


Figure S15. High-resolution mass spectrum of DPD TE.

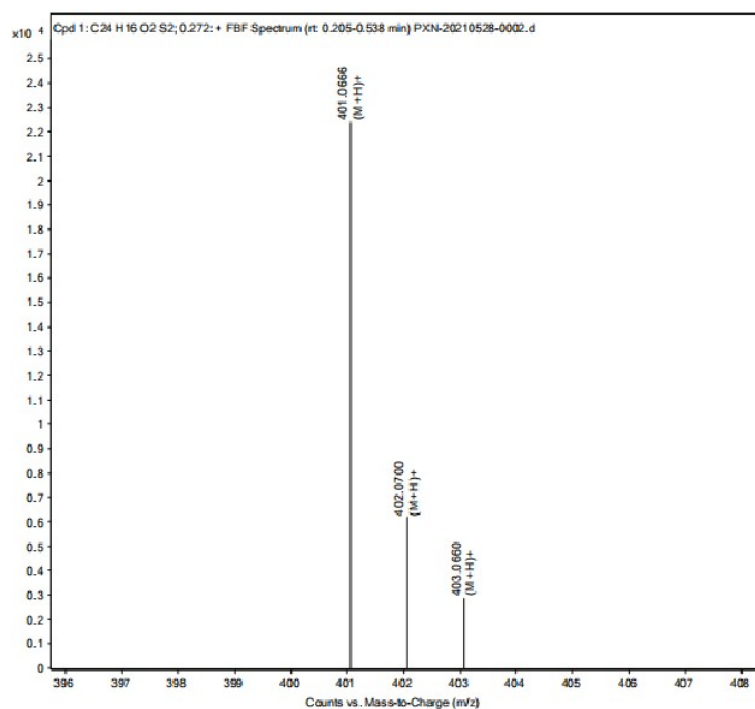


Figure S16. High-resolution mass spectrum of DPDFTE.

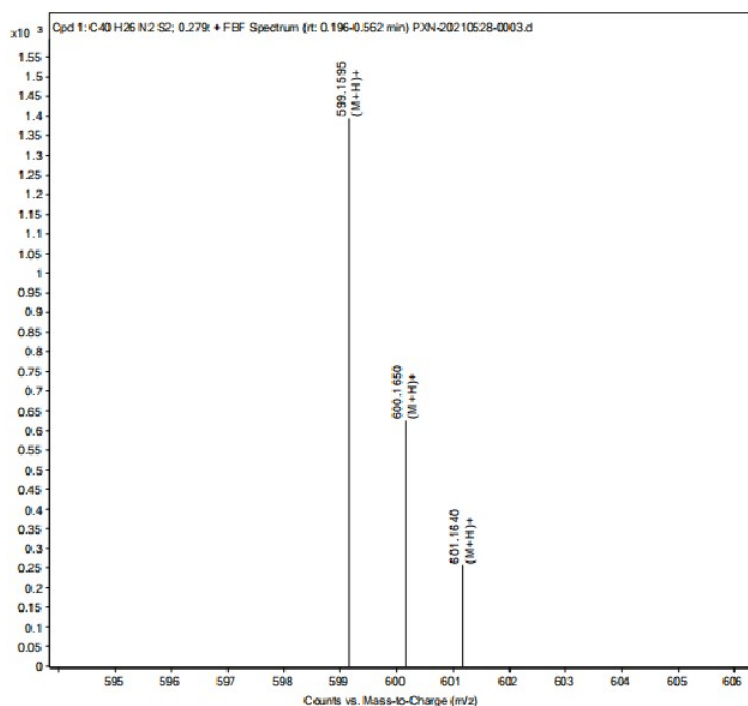


Figure S17. High-resolution mass spectrum of DPDPTE.

5. Reference

- (1) Frisch, M. J.; Trucks, G. W.; Schlegel, H. B.; Scuseria, G. E.; Robb, M. A.; Cheeseman, J. R.; Scalmani, G.; Barone, V.; Mennucci, B.; Petersson, G. A.; Nakatsuji, H.; Caricato, M.; Li, X.; Hratchian, H. P.; Izmaylov, A. F.; Bloino, J.; Zheng, G.; Sonnenberg, J. L.; Hada, M.; Ehara, M.; Toyota, K.; Fukuda, R.; Hasegawa, J.; Ishida, M.; Nakajima, T.; Honda, Y.; Kitao, O.; Nakai, H.; Vreven, T.; Montgomery, J. A., Jr.; Peralta, J. E.; Ogliaro, F.; Bearpark, M.; Heyd, J. J.; Borthers, E.; Kudin, K. N.; Staroverov, V. N.; Kobayashi, R.; Normand, J.; Rahavachari, K.; Rendell, A.; Burant, J. C.; Iyengar, S. S.; Tomasi, J.; Cossi, M.; Rega, N.; Millam, J. M.; Klene, M.; Knox, J. E.; Cross, J. B.; Bakken, V.; Adamo, C.; Jaramillo, G.; Gomperts, R.; Stratmann, R. E.; Yazyev, O.; Austin, A. J.; Cammi, R.; Pomelli, C.; Ochterski, J. W.; Martin, R. L.; Morokuma, K.; Zakrzewski, V. G.; Voth, G. A.; Salvador, P.; Dannenberg, J. J.; Dapprich, S.; Daniels, A. D.; Farkas, O.; Foresman, J. B.; Ortiz, J. V.; Cioslowski, J.; Fox, D. J. Gaussian, Inc. Wallingford CT, 2009.
- (2) Becke, A. D. Density-functional thermochemistry. III. The role of exact exchange. *J. Chem. Phys.* **1993**, *98*, 5648–5652.
- (3) Adamo, C.; Jacquemin, D. The calculations of excited-state properties with time-dependent density functional theory. *Chem. Soc. Rev.* **2013**, *42*, 845–856.